NAVAL POSTGRADUATE SCHOOL
Monterey, California

THESIS

HOLOGRAPHIC INVESTIGATION OF
SOLID PROPELLANT COMBUSTION

by

Albert George Butler

December 1988

Thesis Advisor: David W. Netzer

REPORT DOCUMENTATION PAGE

REPORT SECURITY CLASSIFICATION UNCLASSIFIED	1b RESTRICTIVE MARKINGS
SECURITY CLASSIFICATION AUTHORITY	3 DISTRIBUTION/AVAILABILITY OF REPORT Approved for public release; distribution is unlimited
DECLASSIFICATION/DOWNGRADING SCHEDULE	
ERFORMING ORGANIZATION REPORT NUMBER(S)	5 MONITORING ORGANIZATION REPORT NUMBER(S)
NAME OF PERFORMING ORGANIZATION val Postgraduate School	6b OFFICE SYMBOL (If applicable) Code 67
7a NAME OF MONITORING ORGANIZATION Naval Postgraduate School	
ADDRESS (City, State, and ZIP Code) nterey, California 93943-5000	7b ADDRESS (City, State, and ZIP Code) Monterey, California 93943-5000
NAME OF FUNDING/SPONSORING ORGANIZATION Air Force stronautics Laboratory	8b OFFICE SYMBOL (If applicable)
9 PROCUREMENT INSTRUMENT IDENTIFICATION NUMBER	
ADDRESS (City, State, and ZIP Code) dwards Air Force Base alifornia 93523	10 SOURCE OF FUNDING NUMBERS PROGRAM ELEMENT NO PROJECT NO F04611-88-X0021 TASK NO WORK UNIT ACCESSION NO

TITLE (Include Security Classification)

OLOGRAPHIC INVESTIGATION OF SOLID PROPELLANT COMBUSTION

PERSONAL AUTHOR(S)
utler, Albert G.

TYPE OF REPORT	13b TIME COVERED	14 DATE OF REPORT (Year, Month, Day)	15 PAGE COUNT
aster's Thesis	FROM _____ TO _____	1988, December	56

SUPPLEMENTARY NOTATION
e views expressed in this thesis are those of the author and do not reflect the official
icy or position of the Department of Defense or the U.S. Government.

COSATI CODES			18 SUBJECT TERMS (Continue on reverse if necessary and identify by block number)
FIELD	GROUP	SUB-GROUP	Holography; Solid Propellant; Speckle

ABSTRACT (Continue on reverse if necessary and identify by block number)

An investigation into the behavior of aluminized solid propellant combustion in a two-mensional windowed rocket motor was conducted using holographic techniques. Holograms re recorded in the motor port, aft of the propellant grain and at the entrance to the haust nozzle for two different propellant compositions at varying operating pressures. uantitative particle size data for particles larger than 20 microns were obtained from the lograms. From these data, the mean diameters (D_{32}) of the larger particles were lculated and utilized to compare what effects pressure, location in the motor and uminum content had on the behavior of the aluminum/aluminum oxide particles. D_{32} was und to decrease with increasing pressure, but was unaffected by variations in low values propellant aluminum loading. D_{32} at the grain exit was found to be significantly less an within the grain port.

DISTRIBUTION/AVAILABILITY OF ABSTRACT ☒ UNCLASSIFIED/UNLIMITED ☐ SAME AS RPT ☐ DTIC USERS	21 ABSTRACT SECURITY CLASSIFICATION Unclassified
NAME OF RESPONSIBLE INDIVIDUAL rof. David W. Netzer	22b TELEPHONE (Include Area Code) (408) 646-2980 22c OFFICE SYMBOL Code 67Nt

FORM 1473, 84 MAR 83 APR edition may be used until exhausted
All other editions are obsolete

SECURITY CLASSIFICATION OF THIS PAGE

☆ U.S. Government Printing Office 1986—606-243

Approved for public release; distribution is unlimited

Holographic Investigation of Solid Propellant Combustion

By

Albert George Butler
Lieutenant, United States Navy
B.S., Rensselaer Polytechnic Institute, 1982

Submitted in partial fulfillment of the
requirements for the degree of

MASTER OF SCIENCE IN ENGINEERING SCIENCE

from the

NAVAL POSTGRADUATE SCHOOL
December 1988

ABSTRACT

An investigation into the behavior of aluminized solid propellant combustion in a two-dimensional windowed rocket motor was conducted using holographic techniques. Holograms were recorded in the motor port, aft of the propellant grain and at the entrance to the exhaust nozzle for two different propellant compositions at varying operating pressures. Quantitative particle size data for particles larger than 20 microns were obtained from the holograms. From these data, the mean diameters (D_{32}) of the larger particles were calculated and utilized to compare what effects pressure, location in the motor and aluminum content had on the behavior of the aluminum/aluminum oxide particles. D_{32} was found to decrease with increasing pressure, but was unaffected by variations in low values of propellant aluminum loading. D_{32} at the grain exit was found to be significantly less than within the grain port.

TABLE OF CONTENTS

I. INTRODUCTION ---------- 1

II. EXPERIMENTAL APPARATUS ---------- 5

A. BACKGROUND ---------- 5

B. EQUIPMENT ---------- 5

III. EXPERIMENTAL PROCEDURE ---------- 12

A. SYSTEM CALIBRATION ---------- 12

B. PRE-FIRING PREPARATION ---------- 13

C. FIRING SEQUENCE ---------- 14

D. HOLOGRAM PROCESSING ---------- 15

E. HOLOGRAM RECONSTRUCTION ---------- 16

IV. DISCUSSION OF RESULTS ---------- 18

V. CONCLUSION AND RECOMMENDATIONS ---------- 24

APPENDIX A: TABLES ---------- 27

APPENDIX B: FIGURES ---------- 30

APPENDIX C: COMPUTER PROGRAM ---------- 42

LIST OF REFERENCES ---------- 45

INITIAL DISTRIBUTION LIST ---------- 47

LIST OF TABLES

I. PROPELLANT COMPOSITION ---------- 27

II. SUMMARY OF TEST CONDITIONS AND D_{32} ---------- 28

III. SUMMARY OF PARTICLE SIZE PERCENTAGES ---------- 29

LIST OF FIGURES

2.1 Pulsed Ruby Recording Laser ---------- 30

2.2 Holocamera and Two-Dimensional Motor ---------- 31

2.3 Hologram Reconstruction Apparatus ---------- 31

2.4 Two-Dimensional Motor ---------- 32

2.5 Two-Dimensional Motor Combustion Chamber -------- 32

3.1 USAF Resolution Bar Target ---------- 33

3.2 Reconstructed Hologram of USAF Resolution Bar Target ---------- 33

3.3 Resolution Particle Target ---------- 34

3.4 Reconstructed Hologram of Resolution Particle Target ---------- 34

3.5 Pressure-Time Trace ---------- 35

4.1 Reconstructed Hologram of DD-1 in Motor Port at 162 Psi ---------- 36

4.2 Reconstructed Hologram of DD-5 in Motor Port at 220 Psi ---------- 36

5.1 Particle Size Distribution for DD-1 in Motor Port ---------- 37

5.2 Particle Size Distribution for DD-5 in Motor Port ---------- 38

5.3 Particle Size Distribution for DD-1 and DD-5 Aft of the Propellant Grain ---------- 39

5.4 Particle Size Distribution for DD-1 in Exhaust Nozzle ---------- 40

5.5 Particle Size Distribution for DD-5 in Exhaust Nozzle ---------- 41

ACKNOWLEDGMENTS

I would like to thank Prof. D.W. Netzer for his help and guidance during this undertaking and Harry Conner for the support provided, which made everything a little easier. In addition, I would like to thank my wife and daughter for all their support and understanding while working on this project.

I. INTRODUCTION

Metallized solid propellants used in rocket motors provide increased performance, deliver a higher specific impulse than the non-metallized base propellant and increase propellant density. In particular, the use of aluminum as a metallized additive provides these characteristics while causing only minor changes in the burning rate of most propellants. However, these advantages are not without problems. Primarily, a lower specific impulse efficiency occurs due to the presence of condensed metal oxides in the flow.

Combustion of aluminum does not always occur in the gas phase far from the parent particle, resulting in the formation of very small condensed aluminum oxide particles. Aluminum oxide, having a higher melting temperature than aluminum, produces an oxide film or shell. If this oxide layer is not broken, aluminum vapor must diffuse through the liquid oxide layer and then burn with oxygen in a detached diffusion flame. Particles smaller than two microns play a major role in the exhaust signature while particles greater than five microns can cause significant two-phase flow losses in the exhaust nozzle [Ref. 1:p. 1]. These larger particle sizes are due to the agglomeration of many smaller particles on the propellant burning surface. After breaking

from the surface the agglomerates may require a time of ten to 100 ms to complete burning, and the combustion of the metal does not contribute to the propellant burning rate because the heat released is far from the propellant surface [Ref. 2:p. 480]. These agglomerates, or their oxide caps, also exhibit temperature and velocity lag in the exhaust gas flow and are often the primary reason for the reduction in specific impulse efficiency [Ref. 3:p. 9]. This two-phase flow loss is highly dependent on the particle size distribution of the aluminum and the aluminum oxide entering the exhaust nozzle. The original particle size of the aluminum in the propellant and the subsequent formation of aluminum oxide agglomerates at different operating pressures and temperatures, can affect the overall performance of the metallized solid propellant.

Knowledge of the history of the particles, from the propellant grain surface to the exhaust nozzle, helps enhance the analytical modeling of the combustion process, the prediction of the performance levels of the propellant, and the accuracy of pressure oscillation damping analysis [Ref. 4:p. 2]. Non-intrusive techniques available for studying particular behavior include light scattering, high speed motion pictures and holography.

The holographic investigation is unique in that both amplitude and phase information is obtained. The amplitude information provides a conventional picture and the phase

information enables it to be reconstructed as a three-dimensional image, showing the entire depth of field of the combustion process. Pulsed holography allows a single instant of the dynamics of the combustion process to be recorded. Particle size distributions can then be extracted either manually or by using a computer based technique of automated data retrieval.

Particle size distribution data retrieved from the holograms taken in both the combustion chamber and the exhaust nozzle for various propellant compositions and operating pressures provide a history of the particles in the combustion process. Breakup of large agglomerates, if formed, must take place, otherwise the fraction of unburned aluminum would be very large. This would produce an unsatisfactory specific impulse efficiency due to the aluminum being poorly utilized [Ref. 5:p. 3].

Flame envelopes surrounding the burning particles and smoke (submicron metal oxide) generation during the combustion process are major obstacles to acquiring good quality holograms. Narrow pass filters located between the holographic plate and the scene eliminates the visible flame envelopes. High obscuration due to the smoke generation can prevent the laser from penetrating the scene, resulting in no hologram. Also a reference beam to scene beam illumination ratio of between 4:1 and 10:1 is required to obtain a good quality hologram. Nuetral density filters,

placed in the scene beam for collimated type transmission holograms or in the reference beam for diffuse type holograms, are used to achieve the required ratio [Ref. 6: p. 19].

Diffuse scene illumination is used to reduce or eliminate the schlieren effects produced by temperature and density variations of the combustion gas and burning metal particles [Ref. 7:p. 11]. This diffuse illumination causes speckle in the reconstructed image. Speckle is the granular interference pattern superimposed on a coherent image and it produces spots in the background, which cannot be readily distinguished from the real particles [Ref. 6:p. 41]. This effect hinders the sizing of smaller particles, since the speckle can have a maximum size comparable to the particles at the lower end of the particle size distribution [Ref. 1:pp. 46-47].

The objective of this investigation was to obtain good quality holograms within the motor port, aft of the propellant grain and at the entrance of the exhaust nozzle at various pressures and with varying amounts of aluminum. Particle size distribution data could then be obtained either manually or through the use of computer aided automatic data retrieval, allowing for a comparative study of the effects of pressure in the motor and propellant aluminum content.

II. EXPERIMENTAL APPARATUS

A. BACKGROUND

A two-dimensional windowed rocket motor and a pulsed ruby laser were employed along with a holographic camera to obtain good quality holograms of the combustion process. Initial calibration and alignment of the system was conducted to maximize hologram resolution. Diffuse type transmission holograms, taken to reduce schlieren effects, produced a resolution of approximately eight microns through the windows of the combustion chamber and approximately ten microns through the windows of the exhaust nozzle.

B. EQUIPMENT

1. Laser

A pulsed ruby laser system built by TRW, Inc., under contract to the Air Force Rocket Propulsion Laboratory, was used to provide the illumination for the holocamera. The laser operates at a wavelength of 0.6943 microns and produces an output beam diameter of 3.2 cm. It is composed of a Q-switched oscillator, ruby amplifier, beam expanding telescope, alignment autocollimeter, low power helium-neon pointing laser, coolant system and pump, capacitor bank and power supplies. The laser system is shown in Figure 2.1. The system emits a one joule pulse for 50 nanoseconds or, through a pulse chopping technique, emits a one-quarter

joule pulse for ten nanoseconds. The helium-neon pointing laser (Uniphase, Model 1103P) is incorporated into the laser chest. It is a 1.8 milliwatt, continuous wave laser used for alignment of the pulsed ruby laser. A photodiode also located in the laser chest is used to sense firing of the laser. The laser system is described in detail in References 8 and 9.

Holograms of metallized propellant combustion recorded with a 50 nanosecond pulse show time-averaged fringe effects. By using the ten nanosecond chopped pulse these fringe effects can be reduced [Ref. 10:p. 44]. In the exhaust nozzle, based on the average speeds (Mach = 0.5) achieved in the viewing window, the distance travelled (or time-averaged fringe effect) by a particle was approximately 24 microns for a 50 nanosecond pulse. By chopping the pulse to ten nanoseconds a fringe effect of only 4.8 microns was realized. This was below the resolution limits of the hologram and reduced distortions during reconstruction. In the combustion chamber the average speeds achieved by a particle are much less than in the exhaust nozzle, minimizing any distortions of the particle during reconstruction. Both 50 (in initial tests) and ten nanosecond pulse lengths were used in the exhaust nozzle while only the ten nanosecond pulse length was used in the propellant port and aft of the propellant grain.

2. Holocamera

The holocamera, also built by TRW, Inc., was used to split the laser light into two beams. Using one as the reference beam and passing the other, the scene beam, through the windows of the two-dimensional motor during combustion allowed a hologram to be obtained by the interference pattern formed by recombination of the two beams on the plate. The holographic plates were 4 X 5 inch Afga-Gevaert 8E75 HD glass recording plates. A Uniblitz Model 225 electrical capping shutter was used inside the removable lens-plate box of the holocamera to protect the holographic plate. The shutter was connected to a control box by cables. This allowed for opening of the shutters to coincide with the firing of the laser. The holocamera and the two-dimensional motor are shown in Figure 2.2.

The holocamera is equipped with an opaque diffuser in the scene beam path to eliminate the schlieren effects caused by the burning particles. In addition, an optical filter is contained in the lens-plate box to exclude flame light, but pass the laser light. The holocamera is described in detail in Reference 10.

3. Hologram Reconstruction

After the holographic plate was developed, it was returned to the removable lens-plate box and placed on a stand of an observation microscope. A Spectra Physics Model 165-11 Krypton-ion CW gas laser provided the rear

illumination of the developed hologram. The laser had an output of 500 milliwatts at a wavelength of 0.6471 microns. The holographic plate was placed at an angle of approximately 60 degrees with the laser. The hologram was then reconstructed on a rotating mylar disc placed at the focal point of a variable power observation microscope. This process reduced speckle during reconstruction. The reconstruction laser system is shown in Figure 2.3. Photographs of the reconstruction scene were taken using either a 35 mm or Polaroid camera.

Use of the same laser for both taking and reconstructing the hologram should yield the best resolution due to increased coherence. The use of the pulsed ruby laser for taking holograms allowed for better penetration of the smoke generated by combustion in the motor than the krypton-ion laser, and it provided the stop action required for the moving particles. However, the use of the continuous wave krypton-ion CW laser is required for viewing the reconstructed holograms. The use of these two different lasers, with only small differences in wavelength, provides the best system for obtaining good quality holograms with only minor degredation in resolution.

4. Two-Dimensional Motor

The two-dimensional motor was designed to approximate the flow environment of an actual motor. The flat block design was configured with two sets of high

quality glass window ports, with diameters of 0.343 inches, to allow for laser beam passage through the motor. It was mounted and fired vertically for use with the holocamera. The motor is shown in Figure 2.4. Figure 2.5 shows the combustion chamber of the motor.

The combustion chamber of the motor was 10.5 inches long, 2.3 inches wide and 0.25 inches thick (in the viewing direction). An opposed slab configuration was used for the propellant. Spacers were used, at times, to allow slabs of less then five inches in length to be viewed through the larger of the two sets of window ports. This larger window port was located in the combustion chamber and provided a means of taking holograms just off of the propellant surface. The smaller of the two sets of window ports were located at the end of the combustion chamber and also covered the area at the entrance to the exhaust nozzle. Either set of window ports could be supplied with a nitrogen purge during firing to help protect them. The purge was sonically choked upstream of the windows to provide a fixed mass flow rate of nitrogen to the windows. If the mass flow rate was too high the purge would be introduced into the combustion chamber with high velocity and interfere with the flow of particles. A sonic choke of 0.031 inches diameter was used during the investigation, providing a purge flow rate of approximately 0.00225 lbm/sec.

Ignition of the propellant was accomplished using an igniter filled with $BKNO_3$, located at one end of the combustion chamber. A resistance wire inside the igniter was heated with 12 VDC, firing the $BKNO_3$. Hot gases from the igniter in turn ignited both sides of the opposing slabs of propellant. The nozzles were designed to ensure sonic flow was reached and to provide the desired operating pressures.

5. Propellants

Two propellants, DD-1 and DD-5, were provided by the Air Force Astronautics Laboratory. Both were aluminumized solid propellants with DD-1 having an aluminum content of 2.0% and DD-5 having an aluminum content of 4.69%. The full compositions of both propellants are listed in Table I.

All propellant slabs were loaded using a silicon rubber filler (General Electric RTV-106-Red, High Temperature) as a bonding agent and inhibitor between the motor surfaces and the propellant. Only the propellant surfaces not against the motor (the two opposing sides facing inward and the ends facing the nozzle) were not inhibited. Uninhibited ends were used so that inhibitor products during combustion were kept to a minimum.

Propellant slabs were cut into uniform widths (0.75 inches) and thicknesses (0.25 inches) with varying lengths. By increasing the length, the burning area of the propellant was increased, and the pressure obtained was also increased.

6. Data Acquisition

Operation of the laser system during the two-dimensional rocket motor firing sequence was carried out by automated means using a computer program on a Hewlett-Packard 9836S and an HP data acquisition system. Initial firing of the igniter was done manually, then the computer program, listed in Appendix C, allowed firing of the laser to occur after a set threshold pressure was reached and a specified time delay was met. A pressure-time trace of the firing run was recorded on a Honeywell Model 1508 visicorder. It also recorded the firing of the laser by means of the photodiode in the laser, pinpointing the exact pressure and time during the run when the hologram was recorded.

III. EXPERIMENTAL PROCEDURE

A. SYSTEM CALIBRATION

Initial calibration of the holographic system was accomplished using the pulsed ruby laser and the two-dimensional motor. Calibration targets were inserted into the combustion chamber of the motor and holograms were taken to determine resolution. The motor was windowed and a diffuser was used in the scene beam to match the system setup of the actual firing runs. Each set of windows in the motor had a different thickness, 0.25 inches for the larger and 0.15 inches for the smaller. This affected the optical path length of the scene beam due to the different index of refraction of the glass windows versus air. The scene beam optical path length must match the reference beam path length to ensure maximum coherence and good resolution in the hologram. This temporal match of beam paths was achieved by adjusting the second scene mirror in the holocamera to compensate for the change in the scene path length due to the windows.

Two calibration targets were used, a 1951 USAF resolution bar target and a Laser Electro-Optics Ltd. calibration standard reticle (RR-50-3.0-0.08-102). Resolution for the USAF target was approximately eight microns for the larger windows and ten microns for the

smaller windows. Figure 3.1 shows a photograph of the USAF target and Figure 3.2 shows a photograph of a reconstructed hologram of the USAF target. The Electro-Optics target, having 23 spherical particle diameters (from five to 93 microns) instead of the rectangular bar shapes, was more realistic since the actual combustion products of metallized propellants are also nearly spherical in shape [Ref. 3:p. 17]. Resolution for this target was approximately 12-15 microns for either set of windows. Figure 3.3 shows a diagram of the Electro-Optics target and Figure 3.4 shows a photograph of a reconstructed hologram of the Electro-Optics target. The size of the speckle in the holograms was the limiting factor in the resolution obtained.

B. PRE-FIXING PREPARATION

Inital preparation of the system included proper set up and a thorough cleaning of the motor and windows. The propellant was cut to a pre-determined length and loaded using red RTV. The motor was then reassembled and a wire was placed on the outside of the exit window. This wire was used to determine if the smoke generated by the combustion was enough to obscure the laser light and prevent recording of a hologram. It was also used as a size reference in the reconstruction process.

The laser and holocamera were then aligned using the Helium-Neon pointing laser. Cross hairs were used to spatially align the scene and reference beams. The motor

was then mounted vertically on the test stand and the system was realigned if necessary. After final alignment the cross hairs were removed, the diffuser was connected and the He-Ne laser turned off. The holocamera was then set up with a holographic plate, electronic shutter, and a narrow pass filter to eliminate the flame envelopes. The electronically operated shutter was connected to the control box, which was set to operate the shutter and fire the laser. The reference beam blocking plate in the holocamera was then pulled open. The computer program was then loaded into the HP-9836S. The program trigger voltage and visicorder scale were obtained using a dead weight tester on the pressure transducer. The pressure transducer was then connected to the motor. Purge nitrogen was connected to the motor and set at a pressure equal to two times the expected combustion pressure plus 200 psi. The ruby laser was turned on and configured for either a ten or 50 nanosecond pulse as described in Reference 9. Finally the igniter, which had been preassembled, was connected to the motor and the system was ready for the motor firing sequence.

C. FIRING SEQUENCE

The firing of the laser was carried out automatically by the computer after a specified threshold pressure was reached and a time delay was met. The threshold pressure was set at 100 psig and a time delay of 0.6 to 0.8 seconds was used to allow time for steady state burning to occur.

Holograms taken before steady state would have an inaccurate particle size distribution due to uneven burning, while those taken afterwards would be subjected to greater smoke obscuration and inhibitor fragments interfering with the desired particle data. After the program was ready, the laser capacitor bank charging control was turned on with a key and the nitrogen purge was turned on. The visicorder was then started and the capacitor bank was charged.

The firing sequence was started manually by applying a voltage to the igniter and firing the $BKNO_3$. This in turn fired the propellant in the motor. When the pressure and the time constraints were met, the computer opened the shutter, which in turn fired the laser. The firing of the laser was sensed by the photodiode and recorded on the visicorder along with a pressure-time trace of the run. The residual voltage on the laser capacitor bank was then discharged manually, and all systems were turned off or returned to normal. A pressure time trace from the visicorder showing the position for laser firing is shown in Figure 3.6.

D. HOLOGRAM PROCESSING

Hologram developing was accomplished by removing the exposed holographic plate in a darkroom aided by a Kodak Safelight. The following steps were used in the process:

1. Immerse in Kodak HRP developer for 15 second intervals until visual inspection under the Safelight showed a slight opacity.

2. Rinse in Kodak Stop Bath for 30 seconds to stop development.

3. Rinse in water for five seconds.

4. Immerse in Kodak Rapid Fix for five minutes to set the image.

5. Rinse in water for ten minutes.

6. Immerse in Kodak Photo-Flo solution for 30 seconds.

7. Allow to air dry two to three hours before reconstructing hologram.

E. HOLOGRAM RECONSTRUCTION

The holograms were reconstructed using the Krypton-Ion laser for rear illumination. The holographic plate was reinserted into the lens-plate box, which was placed onto a stand of an observation microscope. The laser beam and hologram plate were initially aligned with a 60 degree angle between them to pass the beam through the plate at the original scene beam angle. Then a decrease of approximately 9.5 degrees in the angle during reconstruction was used to compensate for the wavelength difference between the ruby and krypton lasers [Ref. 10:p. 42]. Final tuning of the illumination beam angle was accomplished while observing a reconstructed image of a resolution target. The reconstructed hologram was then viewed, either with the variable power microscope directly or by connecting a CCTV camera (Panasonic Model WV-1460) into the microscope and observing the picture on a monitor. A mylar disk connected to the microscope was used to help in focusing and, while

rotating, served to blur the speckle, minimizing its effects on the hologram.

IV. DISCUSSION OF RESULTS

The holographic investigation of aluminized solid propellant combustion resulted in obtaining good quality holograms within the motor port, aft of the propellant grain and at the entrance of the exhaust nozzle. Varying lengths of propellant produced various pressures for each of the two propellant compositions tested. All holograms obtained for data retrieval were recorded at or near the maximum pressure of combustion during the steady state portion of the burn. A summary of the test conditions for these runs is shown in Table II. Examples of reconstructed holograms are shown in Figures 4.1 and 4.2.

Although the resolution obtained from the two calibration targets for diffuse holograms through the microscope was approximately eight to 12 microns, the resolution when viewed on a high quality video monitor via CCTV was limited to approximately 20 microns. The resolution was determined by sizing the speckle in the hologram at an area outside the scene volume of the motor. This limit prevented particle size distribution data at or below 20 microns from being reliable, since the speckle could be mistaken for particles. In addition to being limited by the resolution, smoke (submicron particles) generated during combustion was observed on the holograms.

In the hologram this was apparent as varying background opacity. Qualitatively, the more smoke in the hologram the more small size particles there were, and the more effect it should have on decreasing D_{32} (the Sauter mean diameter) for a given set of test conditions.

Particle size distribution data was obtained manually from the holograms. The holograms were displayed on a video monitor using the observation microscope with a 2X objective lens. This provided a 0.0144 inches squared area for viewing. Determining the center of the motor on the hologram was done by measuring the distance from the wire placed outside the exit window to the motor center (1.55 inches). The wire, if not obscured, was recorded as a known point in the hologram. Backing the microscope off this point the measured distance located the viewed scene in the hologram at the center of the motor. By adjusting the viewing area +/- 0.1 inches from the center, a scene volume of 0.00288 inches cubed for taking data was provided. Approximately 200 of the larger particles were sized from each of the holograms recorded in the motor port and aft of the propellant grain. Approximately 100 particles were sized from those at the entrance of the nozzle. A summary of the data obtained for particle size percentages is shown in Table III.

Calculation of the Sauter mean diameter (D32) from the particle size data was accomplished using

$$D_{32} = \frac{\sum N_i D_i^3}{\sum N_i D_i^2}$$

A summary of the calculated values for D_{32} is shown in Table II. Although only particles larger than 20 microns were considered (since no data was reliable at or below 20 microns) the variations in D_{32} were one means of examining the effects of pressure, location and aluminum content on the larger agglomerate sizes of aluminum/aluminum oxide particles.

The effect of pressure on the size of the agglomerates is shown in Figures 5.1-5.5. As pressure increased the mean diameter decreased, for both DD-1 and DD-5. In the motor port (Figures 5.1 and 5.2), in general, as the chamber pressure (and burning rate) increased, the agglomerates became smaller, in agreement with [Ref. 7:p. 4]. This may have been a direct consequence of the increased burning rate as the chamber pressure increased. This effect was carried through down into the nozzle entrance (Figures 5.4 and 5.5), but the effect of pressure on size was not as apparent in the nozzle as in the motor port.

Examination of the particle size distribution (for the larger particles) for either propellant indicated all particles greater then 100 microns, and most of those greater than 50 microns, were no longer present in the flow at the grain exit or at the entrance to the nozzle.

Considering the DD-1 propellant at approximately 275 psi it is seen that D_{32} was 56 microns within the propellant port (near the head end where t_{res} = 0.22 msec), 46 microns at the grain exit (t_{res} = 0.6 msec) and 44 microns at the nozzle entrance (t_{res} aft of grain = 4.3 msec). The decrease in D_{32} through the grain port could be attributed to the burning of the larger particles, or to the deformation and break up of the larger particles. The Mach number within the propellant port for these conditions was approximately 0.16. A good correlation parameter for the deformation and break up of the agglomerates is the Weber number, which is the ratio of inertial forces to surface tension forces. It is also directly proportional to the square of the velocity lag of the agglomerates. At Weber numbers less then four, the aluminum oxide is spherical, but distorts for Weber numbers greater then four. Breakup usually occurs for Weber numbers between 12 and 20 [Ref. 7:pp. 2-3]. As the Mach number of the flow reaches about 0.08 all agglomerates greater then 1000 microns begin to break up. At a Mach number equal to 0.1 those at 500 microns break up and at a Mach number equal to 0.5 those at 200 microns break up. In the grain port at 275 psi the Mach number was approximately 0.16, whereas, aft of the grain it was only 0.04. Thus, there was little change in particle size from the grain exit to the nozzle entrance.

In addition to the effects of pressure and location, the effect of propellant aluminum loading was investigated. A comparison of the propellants showed that with an aluminum content between 2.0% and 4.69%, there was no significant effect on D_{32}. Qualitatively there were larger amounts of smoke present for DD-5, then for DD-1.

Investigation of the flowfield from the scene volume indicated that a majority of the larger agglomerates resided towards the center of the flow. This could be caused by the influence of the nitrogen purge on the area just inside the motor at the location of the windows. By decreasing the nitrogen purge to a level just acceptable for keeping the windows clean, the effect of the purge on the flow was minimized. The nitrogen purge method used for keeping the windows of the two-dimensional motor clean during the runs proved adequate.

Investigation of the inhibitor and particulate deposit patterns in a partially disassembled motor revealed that, at times, uneven burning at the propellant surface was taking place. This was especially noticable at pressures higher then 500 psi, and when rapid rises in pressure (pressure spikes) occurred. Causes for this may have been the uneven ignition of the propellant surface when the igniter fired. Also, the inability of the inhibitor to bond properly to the propellant surface at the higher pressures may have been the cause. The disassembled motor also showed a build-up of

aluminum oxide on the walls of the converging section of the nozzle. A videotape of the exhaust flow from the two-dimensional motor showed periods when the nozzle appeared clogged, afterwhich it then rapidly cleared itself. These results would indicate that the aluminum oxide tended to agglomerate on the nozzle walls, then break up and pass through the nozzle with slight changes in pressure.

The holographic investigation provided data which enabled a history of the larger particles to be constructed as they passed through the motor. Using calculations of D_{32} the effects of pressure, location and aluminum content were investigated. Further investigation of the holograms, using automated data retrieval, would allow for verification of the particle size distributions obtained manually. It may also permit obtaining particle size data down to approximately 15 microns.

V. CONCLUSIONS AND RECOMMENDATIONS

The holographic investigation of aluminized solid propellant provided a means of comparing the effects of pressure, location in the motor (as a function of t_{res}) and aluminum content on the larger size particles formed during combustion. Data, obtained manually from the holograms, provided particle size distribution information and a means for calculating D_{32} (Sauter mean diameter). With D_{32}, although biased towards the larger particle sizes, and a plot of particle size distribution percentage versus pressure, the relative effects were shown. Increases in pressure alone yielded smaller particles within the propellant port. However, only very small decreases in particle sizes due to increased pressure were seen at the entrance to the exhaust nozzle. In addition, an increase in aluminum loading content from 2.0% (DD-1) to 4.69% (DD-5) seemed to have minimal impact on the mean particle size.

The effect of location in the motor had the most impact on the agglomerate size. In the motor port D_{32} for the various test conditions was calculated between 50 and 66 microns. Aft of the propellant grain yielded D_{32} values between 46 and 50 microns, and at the entrance to the exhaust nozzle D_{32} was between 44 and 48 microns. In addition, the 100-150 micron particles observed within the

propellant port were not present at the grain exit. The small calculated residence time for the motor port would support the conclusion that the size decreases were due more to breakup of the agglomerates in the flowfield then to their burning down in size. Also, due to the very low Mach numbers aft of the propellant, the mean particle size, at the nozzle entrance, was independent of test conditions.

Limitation of particle resolution on the reconstructed holograms due to the speckle from the diffuse type holography presented the major obstacle in obtaining more complete particle size distribution data. Although particle size resolution, on an observation microscope, of below ten microns could be achieved, the viewing of the scene on a high quality video monitor (for manual data retrieval) produced speckle sizes on the order of 20 microns. This caused the calculations of D_{32} to be biased towards the larger particle sizes. Smoke generation also caused larger particles to possibly be missed in the manual data retrieval.

Incorporation of a new design for the holocamera, to allow for larger and better optics, could help reduce the speckle size in the reconstructed hologram. Also the two-dimensional motor could be configured with longer nozzles to study the effects of the exhaust nozzle (with its increasing Mach number) on the particle size distribution. Continuing efforts into automatic data retrieval should also

enhance the capability of the holographic technique for studying particle behavior in any combustion apparatus.

APPENDIX A

TABLES

TABLE I

PROPELLANT COMPOSITION

	DD-1	DD-5
AP(200 microns)	47.450%	45.700%
AP(20 microns)	25.550%	24.610%
GAP	14.670%	14.670%
TEGDN	8.490%	8.490%
Aluminum	2.000%	4.690%
N - 100	0.845%	0.845%
HDI	0.845%	0.845%
Tepanol	0.150%	0.150%

TABLE II

SUMMARY OF TEST CONDITIONS AND D32

LOCATION	PROP	LENGTH (in)	MAX Pc (psi)	HOLOGRAM Pc (psi)	PULSE LENGTH (ns)	D32 (microns)
MOTOR PORT	DD-1	3.00	161	161	10	67
	DD-1	4.25	257	250	10	56
	DD-1	5.25	461	423	10	54
	DD-5	3.00	220	220	10	65
	DD-5	5.25	409	409	10	58
	DD-5	4.25	460	436	10	51
AFT OF GRAIN	DD-1	4.50	288	273	10	46
	DD-5	4.50	415	362	10	49
ENTRANCE OF EXHAUST NOZZLE	DD-1	2.25	136	136	50	48
	DD-1	3.25	198	191	50	45
	DD-1	2.75	308	308	50	44
	DD-5	2.25	150	150	50	46
	DD-5	2.75	200	200	50	44
	DD-5	3.25	278	257	10	44

TABLE III

SUMMARY OF PARTICLE SIZE PERCENTAGES

A. MOTOR PORT

SIZE (microns)	DD-1 161psi	DD-1 250psi	DD-1 423psi	DD-5 220psi	DD-5 409psi	DD-5 436psi
25-30	20	26	31	17	26	32
30-40	22	30	32	27	33	35
40-50	31	31	27	32	30	28
50-75	17	9	7	16	6	3
75-100	8	3	2	6	4	1
100-150	2	1	1	2	1	1

B. ENTRANCE OF EXHAUST NOZZLE

SIZE (microns)	DD-1 136psi	DD-1 191psi	DD-1 308psi	DD-5 150psi	DD-5 200psi	DD-5 257psi
25-30	28	36	39	30	32	36
30-40	40	36	37	31	35	37
40-50	24	23	20	28	22	19
50-75	5	3	2	10	11	7
75-100	3	2	2	1	0	1
100-150	0	0	0	0	0	0

C. AFT OF PROPELLANT GRAIN

SIZE (microns)	DD-1 273psi	DD-5 362psi
25-30	29	23
30-40	33	36
40-50	27	30
50-75	10	8
75-100	1	3
100-150	0	0

APPENDIX B

FIGURES

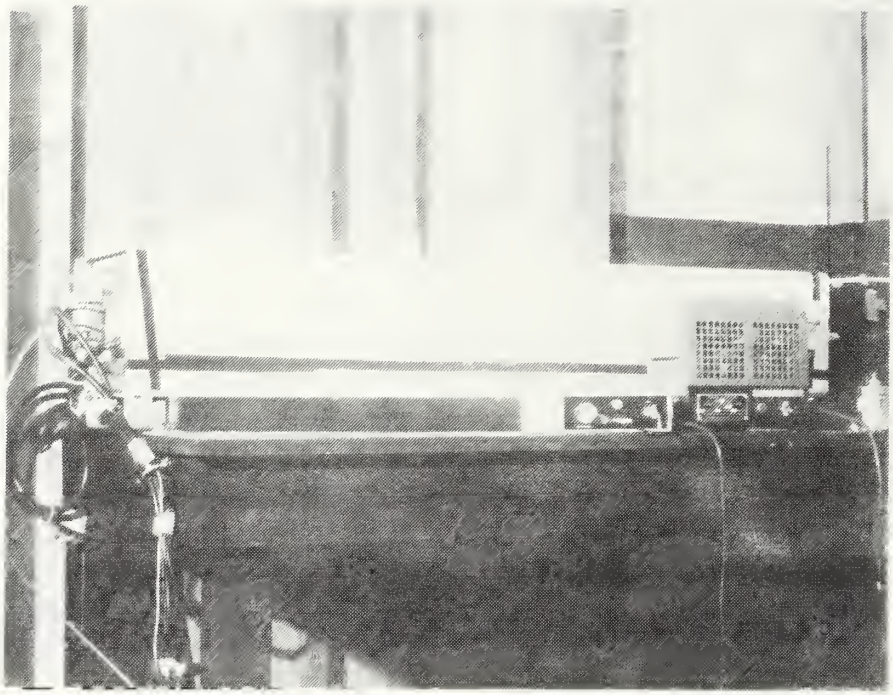

Figure 2.1 Pulsed Ruby Recording Laser

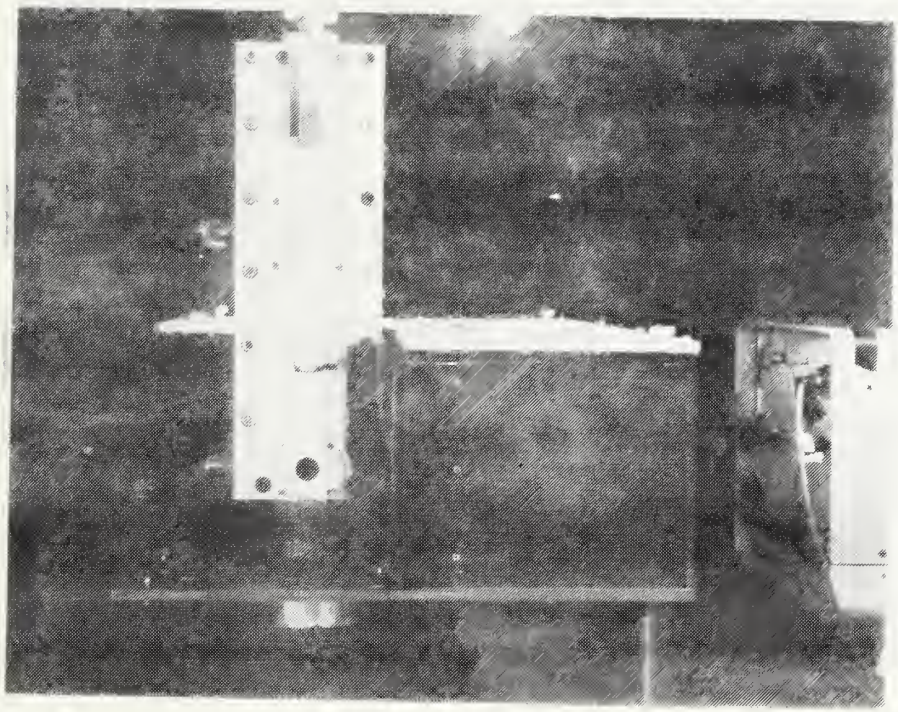

Figure 2.2 Holocamera and Two-Dimensional Motor

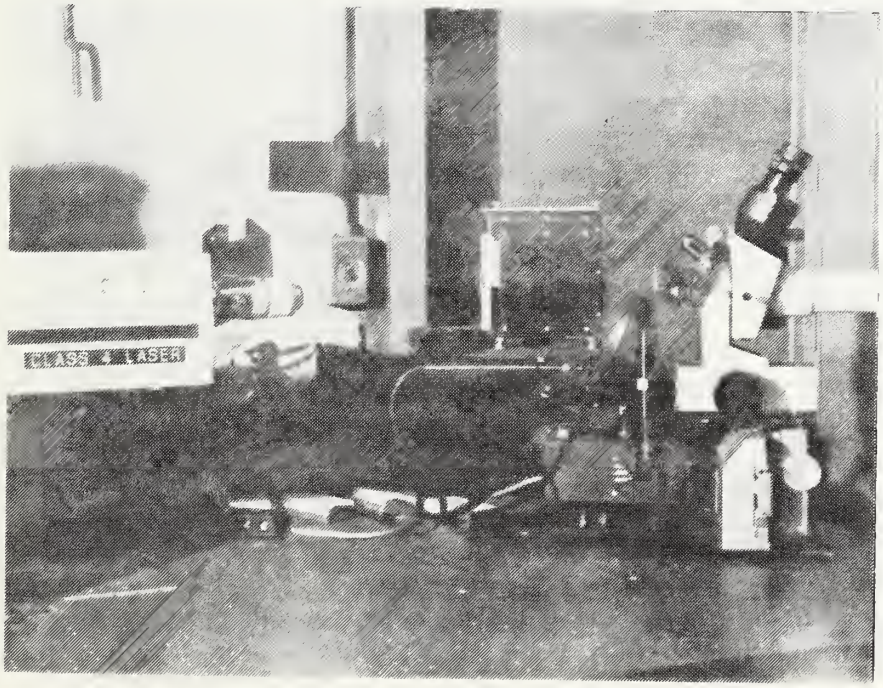

Figure 2.3 Hologram Reconstruction Apparatus

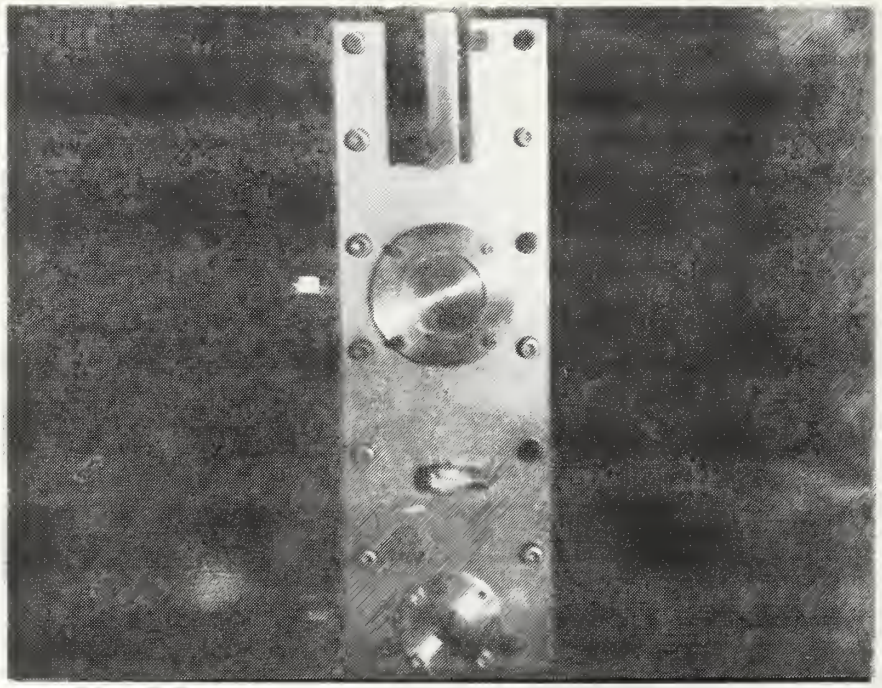

Figure 2.4 Two-Dimensional Motor

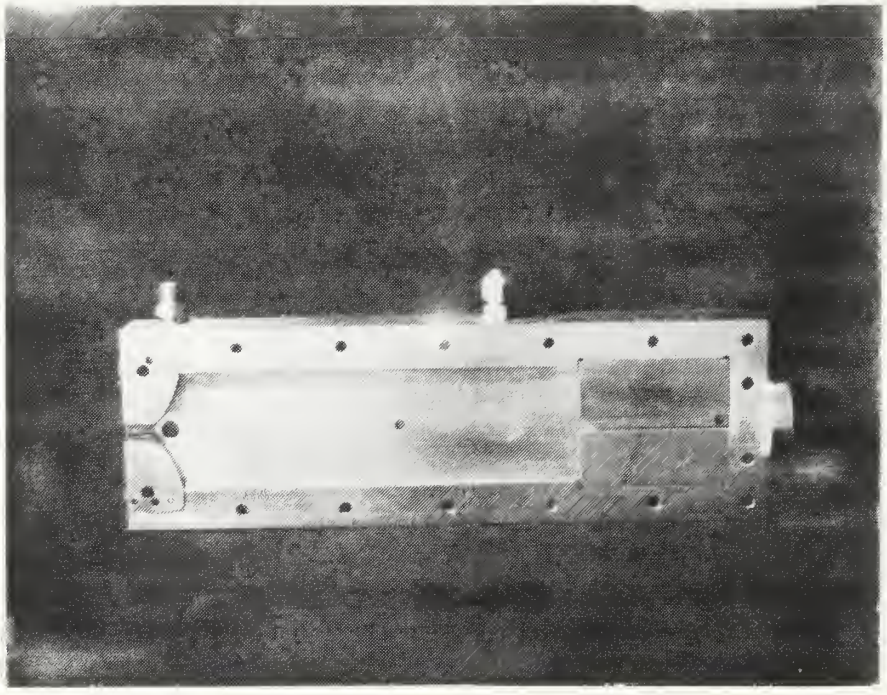

Figure 2.5 Two-Dimensional Motor Combustion Chamber

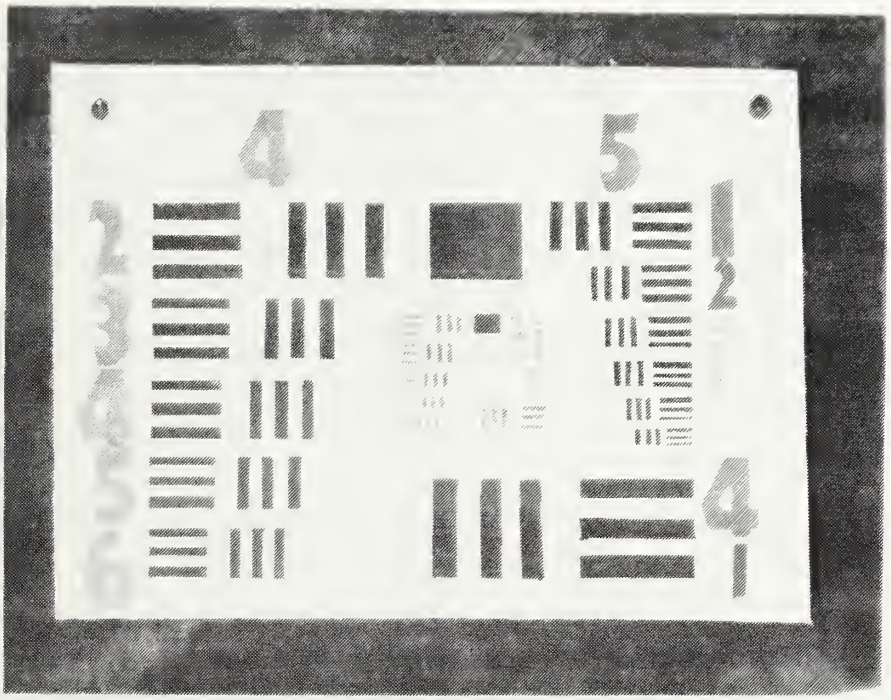

Figure 3.1 USAF Resolution Bar Target

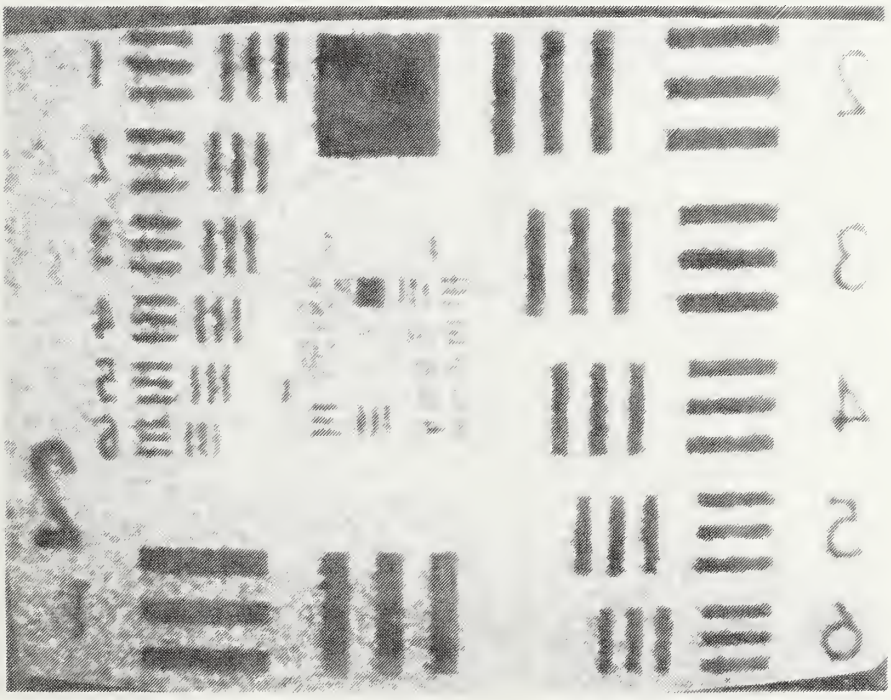

Figure 3.2 Reconstructed Hologram of Resolution Bar Target

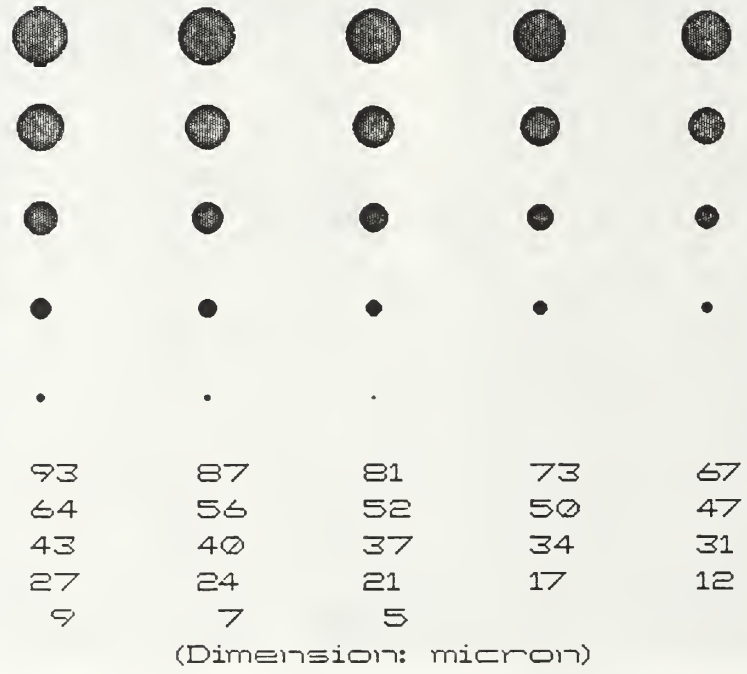

Figure 3.3 Resolution Particle Target

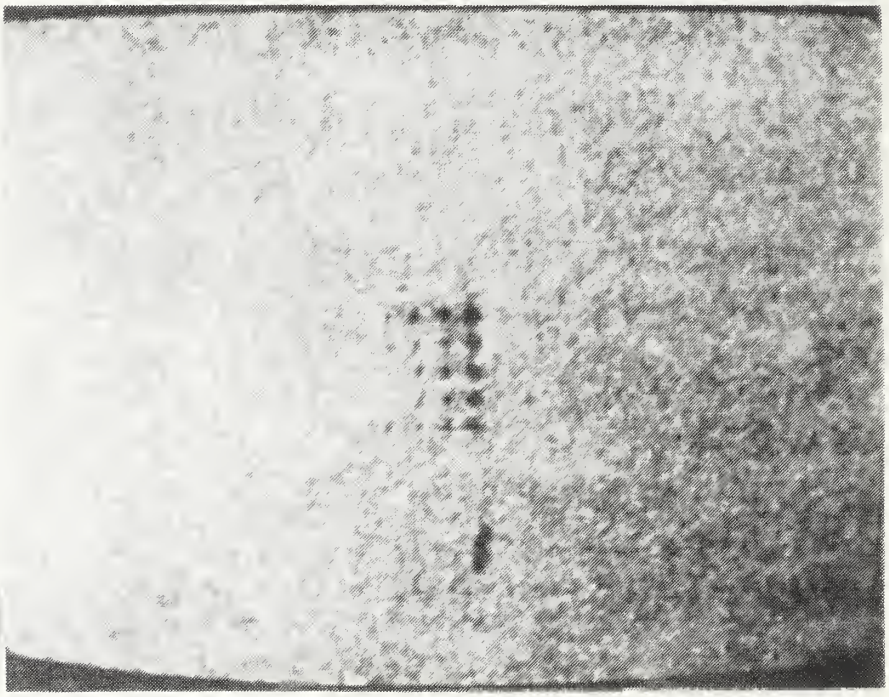

Figure 3.4 Reconstructed Hologram of Resolution Particle Target

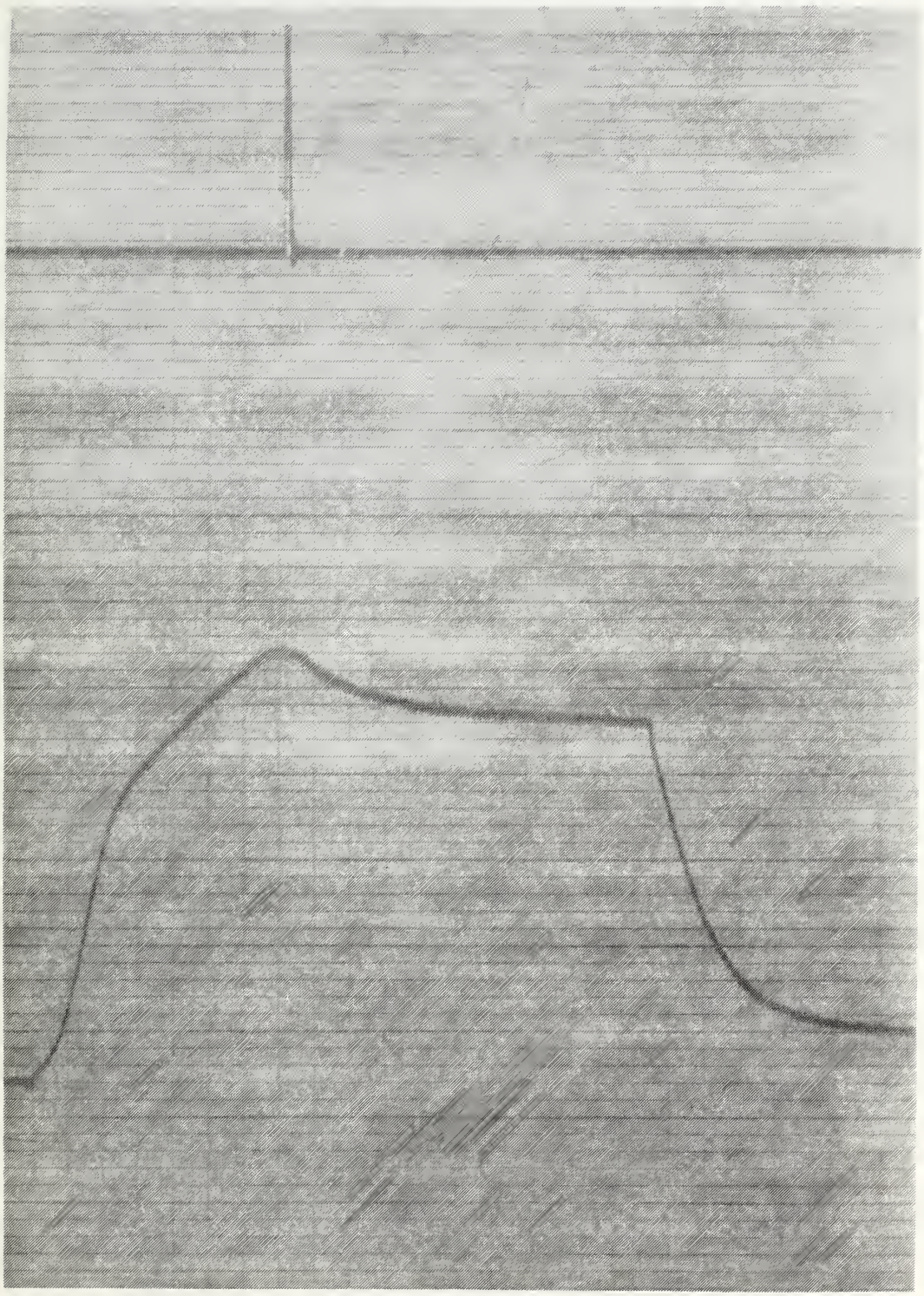

Figure 3.5 Pressure Time Trace

Figure 4.1 Reconstructed Hologram of DD-1 in Motor Port at 162 Psi

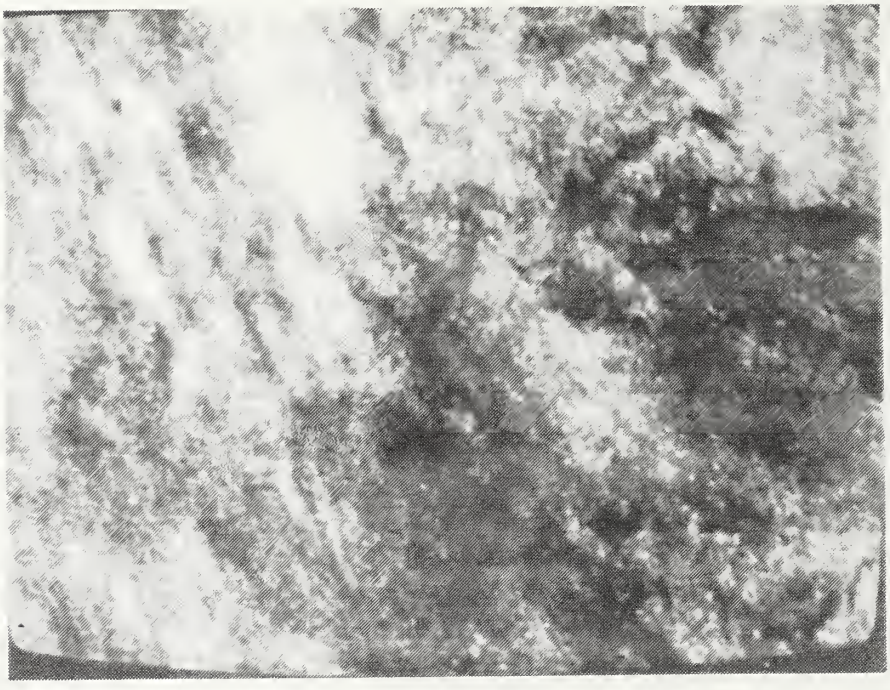

Figure 4.2 Reconstructed Hologram of DD-5 in Motor Port at 220 Psi

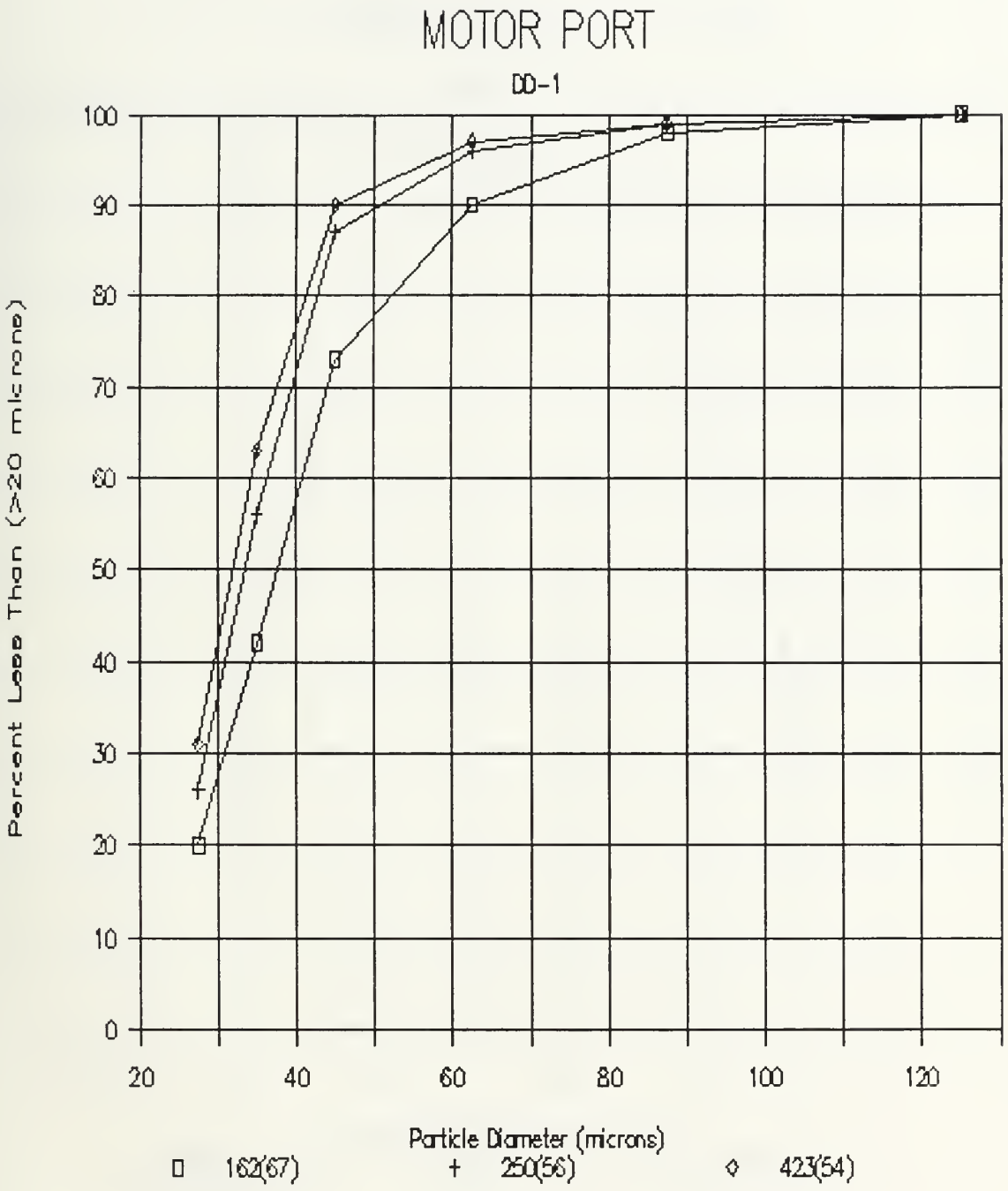

Figure 5.1 Particle Size Distribution for DD-1 in Motor Port

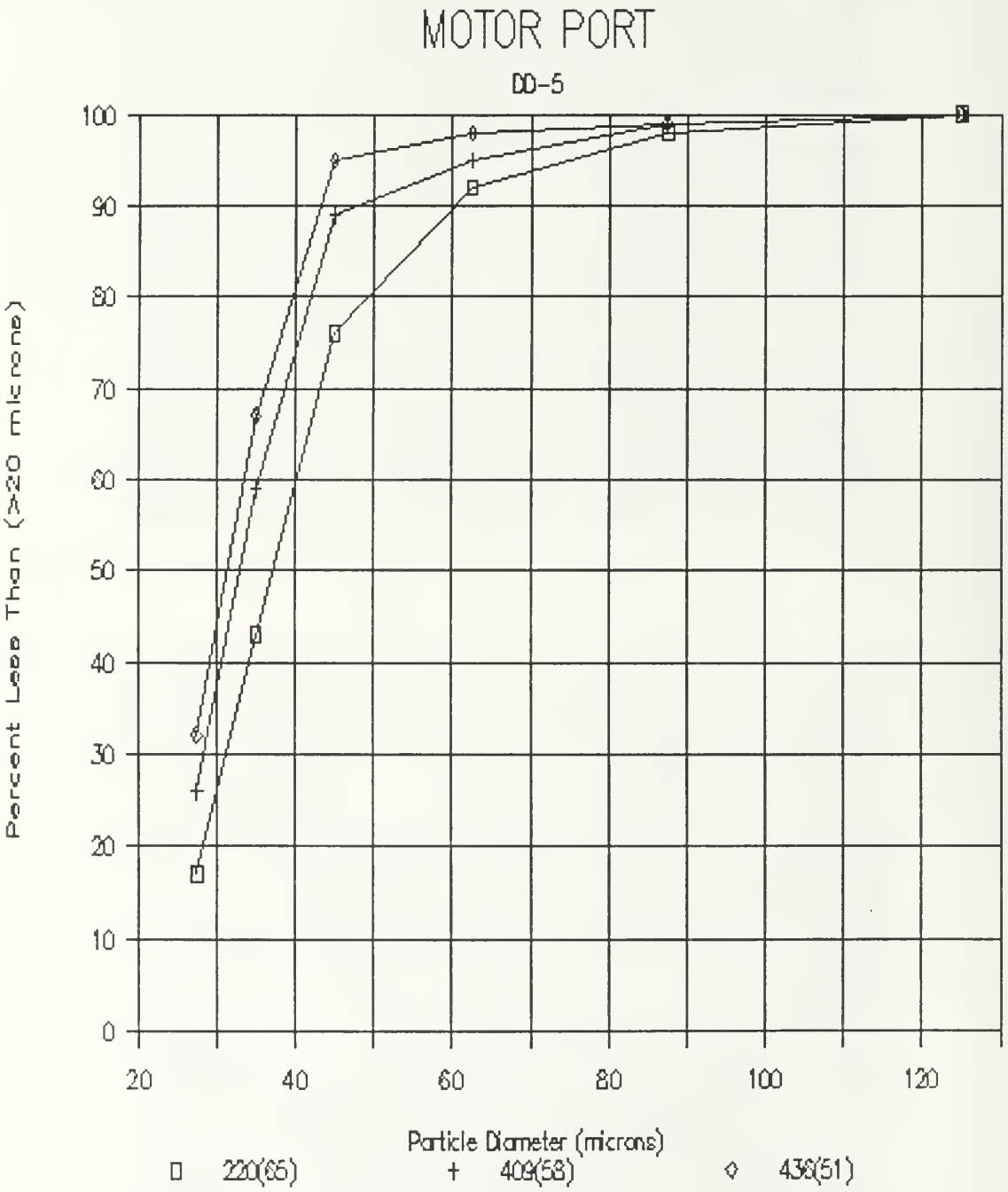

Figure 5.2 Particle Size Distribution for DD-5 in Motor Port

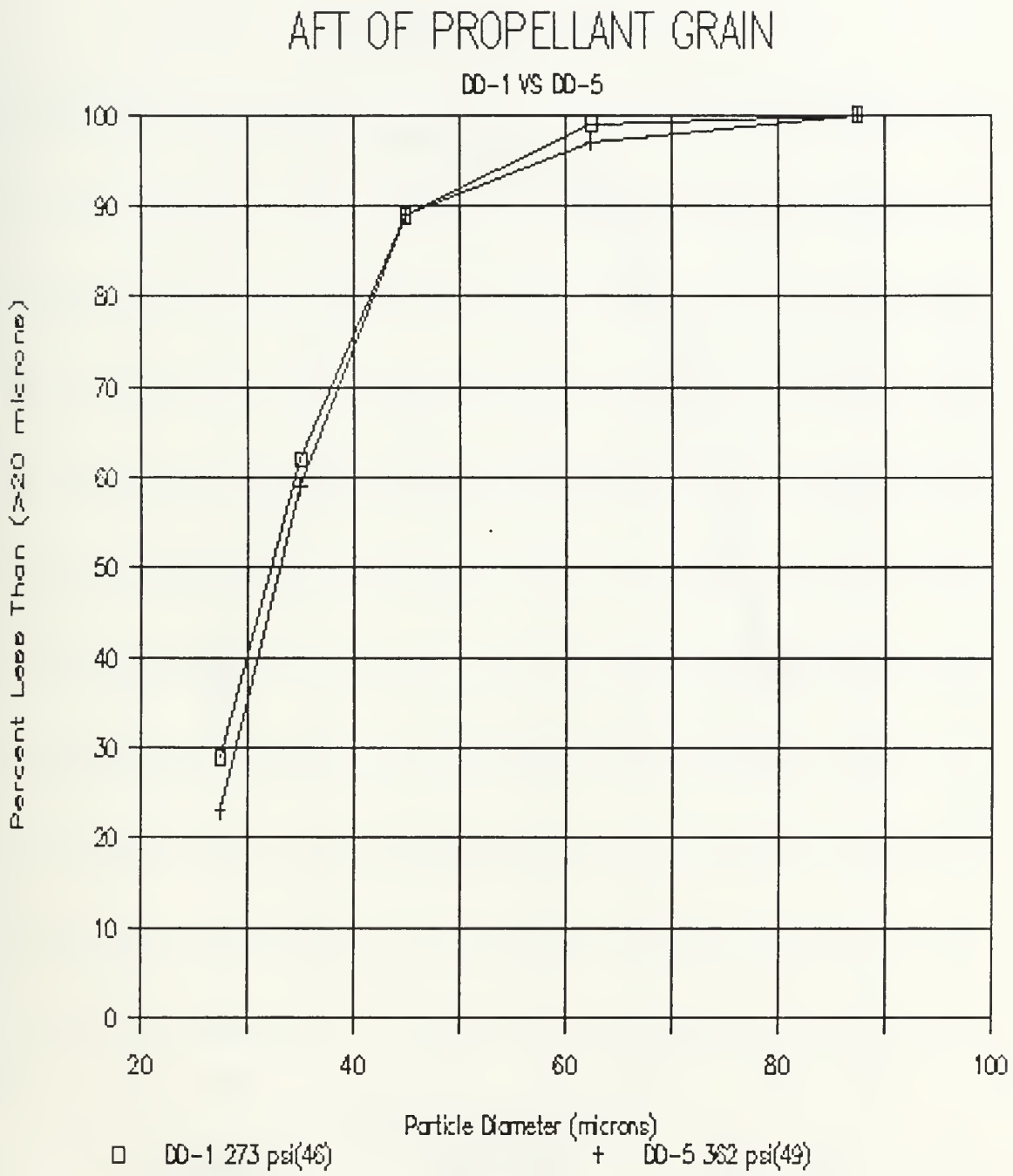

Figure 5.3 Particle Size Distribution for DD-1 and DD-5 Aft of the Propellant Grain

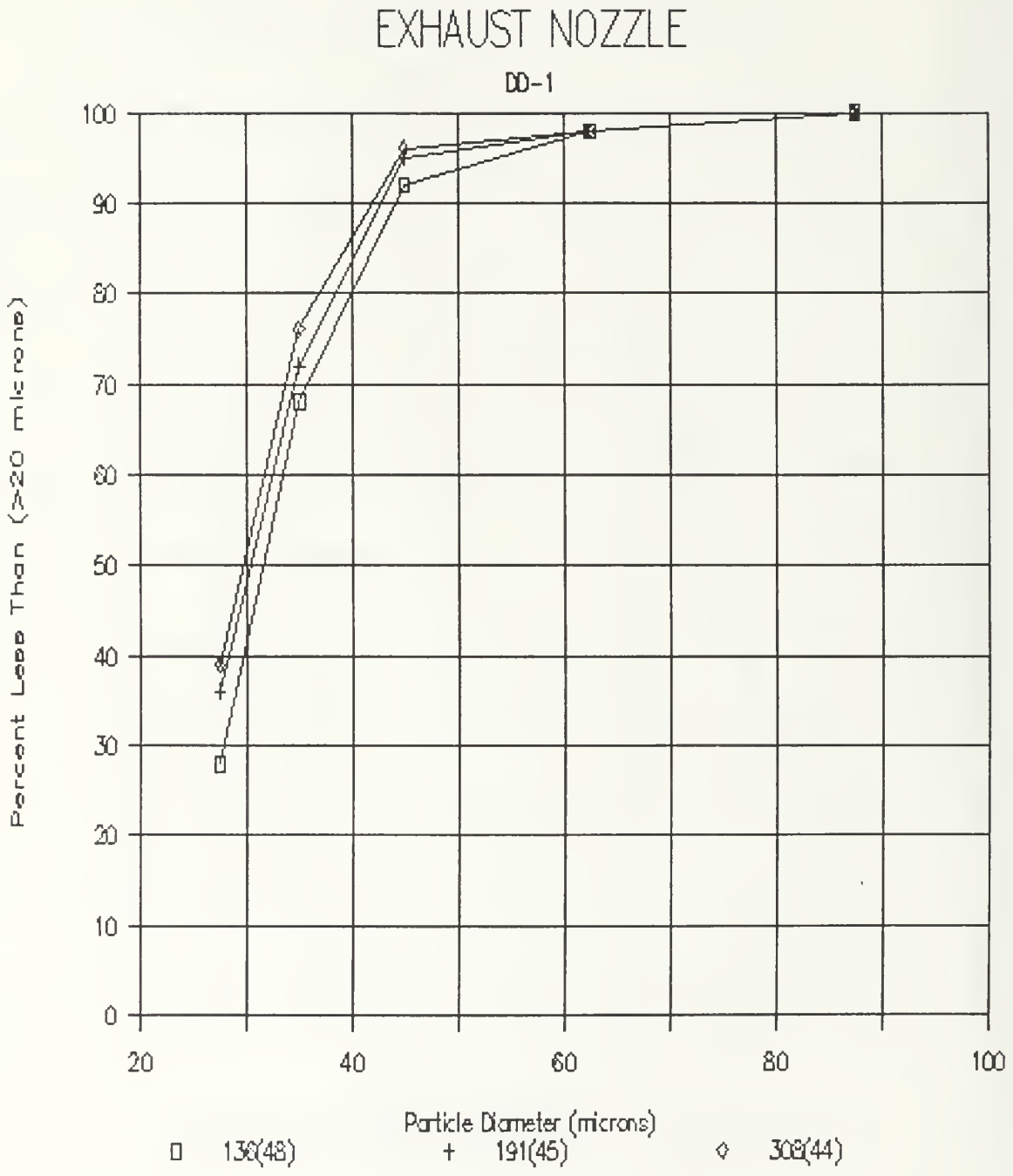

Figure 5.4 Particle Size Distribution for DD-1 in Exhaust Nozzle

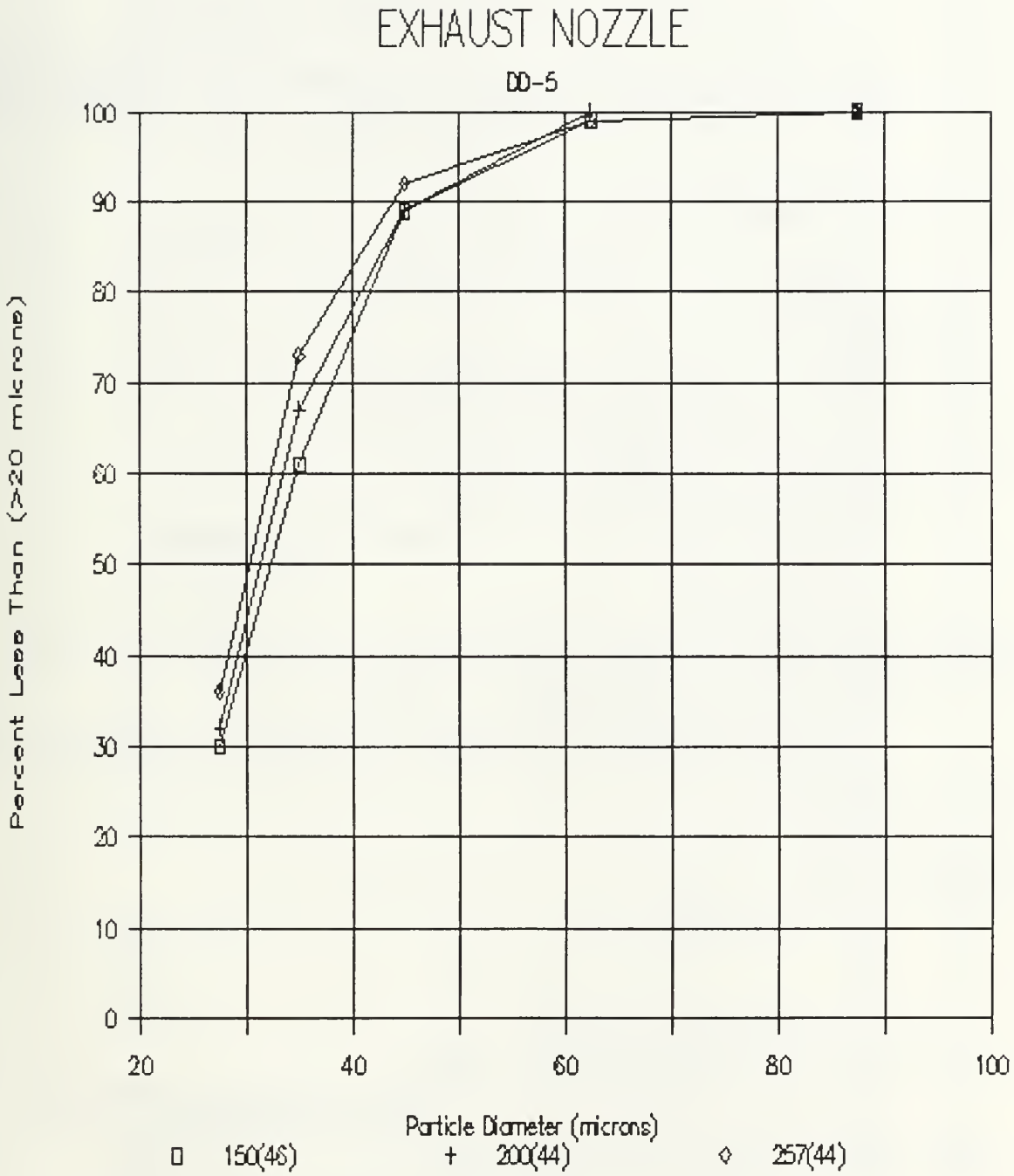

Figure 5.5 Particle Size Distribution for DD-5 in Exhaust Nozzle

APPENDIX C

COMPUTER PROGRAM

```
10        !********** 2-D MOTOR HOLOGRAPHY **********
20    !
30    !THIS PROGRAM IS DESIGNED TO CALIBRATE THE TRANSDUCER SYSTEM
40    !AND THEN SET THE HP-9836S COMPUTER TO FIRE THE AFRPL LASER
50    !SYSTEM AT A DESIRED TRIGGER PRESSURE AND TIME DELAY.
60    !
70    OPTION BASE 1
80    !
90    !THE FOLLOWING SECTION CALIBRATES THE TRANSDUCER.
100   !
110   CLEAR 709          !SET UP 709 AND 722
120   CLEAR 722          !FOR DATA ACQUISITION
130   REMOTE 709
131   REMOTE 722
140   OUTPUT 722;"L1F1R3ISTNZ110STIT4QX1"
141   !L1=LOAD THE FOLLOWING INSTRUCTIONS
142   !F1=DC VOLTS MEASUREMENTS
143   !R3=ONE VOLT RANGE
144   !1STN=ONE READING PER TRIGGER
145   !Z1=AUTO ZERO ON
146   !10STI=10 POWER LINE CYCLES USED FOR INTEGRATION
147   !T4=TRIGGER HOLD
148   !Q=END PROGRAM
149   !X1=WAITING TO BE TRIGGERED
151   INPUT "DO YOU WANT TO CALIBRATE THE TRANSDUCER?(Y/N)"Yy$
160   IF Yy$="N" THEN GOTO 470
170   PRINT "***** ZERO PRESSURE *****"
180   PRINT "INSURE THAT NO PRESSURE IS APPLIED TO THE TRANSDUCER."
190   DISP "HIT CONTINUE WHEN READY TO TAKE ZERO READING."
200   PAUSE
210   REMOTE 709
220   OUTPUT 709;"AC07"
230   WAIT 2
240   OUTPUT 722;"T3"
250   ENTER 722;Vpa0
260   PRINT "Vpa0 =";Vpa0
270   BEEP
280   INPUT "READING OK? (Y/N)",Zz$
290   IF Zz$="N" THEN GOTO 170
300   PRINT USING "@"
310   PRINT "***** CALIBRATION *****"
320   PRINT "APPLY MAXIMUM PRESSURE USING DEAD WEIGHT TESTER."
330   INPUT "ENTER THE MAXIMUM PRESSURE IN Psig",Pmax
340   DISP "HIT CONTINUE WHEN READY"
350   PAUSE
```

```
370   OUTPUT 709;"AC07"
380   WAIT 2
390   OUTPUT 722;"T3"
400   ENTER 722;Vpamax
410   PRINT"Vpamax =";Vpamax,"Pamax =";Pamax
420   Kpa=(Pamax)/(Vpamax-Vpa0)
421   Kpa=ABS(Kpa)
430   PRINT "Kpa ="Kpa
440   BEEP
450   INPUT "READING OK? (Y/N)",Zz$
460   IF Zz$="N" THEN GOTO 300
470   !
480   !THIS SECTION SETS THE SYSTEM UP FOR THE DESIRED CONDITIONS.
490   !
500   CLEAR 709
530   OUTPUT 722;HSM002SW2Z0S01L1FFL0.01STIS0F1R1T3Q"
531   !H RESETS THE DVM
532   !SM002 SETS SERVICE REQUEST MASK WHERE 002 IS OCTAL REP
533   !OF THE SERIAL POLL MASK BYTE
534   !SW2 TELLS WHICH TERMINAL SWITCH IS USED
535   !Z0 IS AUTO ZERO OFF
536   !S01 SYSTEM OUTPUT MODE ON-WAITS FOR CONTROLLER TO HANDSHAKE
537   !L1 LOAD INTERNAL MEMORY ON
539   !0.01STI .01 POWER LINE CYCLES USED FOR INTEGRATION
540   !F1R1 FIRE ONCE READ ONCE
541   !T3 TRIGGER NOW
543   !Q=END PROGRAM
544   PRINT USING "@"
550   INPUT "ENTER THRESHOLD PRESSURE TO TRIGGER DEVICES(Psig)",Pt
560   PRINT "TIMES ARE INTERPRETED BY COMPUTER IN SECONDS TO .001"
561   PRINT "MINIMUM DELAY IS .1 SEC PLUS INPUT TIME DELAY"
570   INPUT "ENTER THE TIME DELAY FROM THRESHOLD PRESSURE(SEC)",T8
580   OUTPUT 709;"AC07"  !CHANNEL FOR CHAMBER PRESSURE
590   WAIT .3   !THIS WAIT IS TO LET VOLTAGES SETTLE DOWN
591   IF Yy$="Y" THEN GOTO740  !IF FULL CAL DONE NO NEW ZERO NEEDED
600   V1=0
610   CLEAR 722  !THIS DOESN'T ALTER INSTRUCTIONS TO THE VOLTMETER
620              !IT CLEARS NUMBERS IN DISPLAY OR OUTPUT REGISTERS
630   FOR I=1 TO 10
640   OUTPUT 722;"T3"      !TRIGGER THE VOLTMETER
650   ENTER 722;V          !READ THE VOLTMETER
660   V1=V1+V
670   NEXT I
680   Vpa0=V1/10           !THIS AVERAGES THE READINGS TO GET A
690                        !ZERO PRESSURE VALUE
700   PRINT USING "40A,D.6D";"   ZERO PRESSURE VOLTAGE=",Vpa0
731   INPUT "ENTER Kpa.",Kpa
732   Kpa=ABS(Kpa)
740   R=Pt/Kpa    !GIVES TARGET VOLTAGE OF PRESSURE TRANSDUCER.
750   PRINT "LASER FIRES WHEN ABS(Vt-Vpa0) EXCEEDS",R
760   PRINT "PLUS TIME DELAY IS MET"
```

```
770   !
780   !THIS SECTION ACTUALLY FIRES THE LASER SYSTEM.
790   !
791   DISP "HIT CONTINUE WHEN THE SYSTEM IS READY TO FIRE"
792   PAUSE
800   PRINT "     BE SURE THE NITROGEN SYSTEM IS ON"
810   PRINT "BE SURE VISICORDER IS SET UP TO RUN ON PROPER SCALE"
811   PRINT "WITH LAMP ON"
820   PRINT USING "/"
840   PRINT "   STANDING BY FOR IGNITION!"
850   BEEP 2000,.1
851   CLEAR 709
852   CLEAR 722
860   OUTPUT 709;"AC07"  !CONNECT THE PRESSURE TRANSDUCER TO DVM
890   OUTPUT 722;"X1"    !TRIGGER THE VOLTMETER
900   ENTER 722;V
901   R1=ABS(V-Vpa0)
902   PRINT "V=",R1
910   IF R1<R THEN GOTO 890 !IF PRESSURE LESS THAN THRESHOLD,REPEAT
920   WAIT T8
930   OUTPUT 709;"DC10,6"   !CLOSES LASER FIRE SWITCH
940   WAIT .5
950   OUTPUT 709;"DO10,6"   !OPENS LASER FIRE SWITCH
960   PRINT "BE SURE TO TURN OFF NITROGEN"
970   PRINT "ENSURE ALL SYSTEMS ARE PROPERLY SHUT DOWN"
980   END
```

LIST OF REFERENCES

1. Air Force Astronautics Laboratory, AFAL-TR-87-029, Measurements of Particulates in Solid Propellant Rocket Motors, by D.W. Netzer and others, October 1987.

2. Price, E.W., "Combustion of Metallized Propellants," Fundamentals of Solid Propellant Combustion, Vol. 90, p. 480, 1984.

3. Yoon, S.C., Holographic Investigation of Solid Propellant Combustion in a Three-Dimension Motor, Master's Thesis, Naval Postgraduate School, Monterey, California, December 1985.

4. Advisory Group for Aerospace Research and Development, AGARD-CP-391, Smokeless Propellants, Experimental Techniques for Obtaining Particle Behavior in Solid Propellant Combustion, by D.W. Netzer and J.P. Powers, November 1985.

5. American Institute for Aeronautics an Astronautics, Breakup of Al/Al2O3 Agglomerates and Accelerating Flow Fields, by L.H. Cavaney and A. Gany, 17th Aerospace Sciences Meeting, 15-17 January 1979.

6. Air Force Rocket Propulsion Laboratory, AFRPL-TR-84-014, An Investigation of Experimental Techniques for Obtaining Particulate Behavior in Metallized Solid Propellant Combustion, by D.W. Netzer and others, February 1984.

7. Rubin, J.B., Holographic Investigation of Metallized Solid Propellant Combustion in a Three-Dimensional Motor, Master's Thesis, Naval Postgraduate School, Monterey, California, September 1986.

8. Air Force Rocket Propulsion Laboratory, TRW Report #11709-6003-R0-00, Instruction Manual for Ruby Laser Holographic Illuminator, by R.F. Wueker, February 1970.

9. Air Force Rocket Propulsion Laboratory, AFRPL-TM-78-11, Instruction Manual for the Improved Ruby Laser Holographic Illuminator, by R.A. Briones and R.F. Wueker, July 1978.

10. Air Force Rocket Propulsion Laboratory, AFRPL-TM-78-12, Operation Manual for Lens-Assisted Multipulse Holocamera with Reflected Light Option, by R.A. Briones and R.F. Wueker, July 1978.

INITIAL DISTRIBUTION LIST

		No. Copies
1.	Defense Technical Information Center Cameron Station Alexandria, Virginia 22304-6145	2
2.	Library, Code 0142 Naval Postgraduate School Monterey, California 93943-5002	2
3.	Professor D.W. Netzer, Code 67Nt Department of Aeronautics and Astronautics Naval Postgraduate School Monterey, California 93943-5000	2
4.	Professor E. Roberts Wood, Code 67Ws Department of Aeronautics and Astronautics Naval Postgraduate School Monterey, California 93943-5000	1
5.	Albert G. Butler 31 Westcliff Drive Mt. Sinai, New York 11766	2

Thesis
B933 Butler
c.1 Holographic investigation of solid propellant combustion.